OPEN ACCESS Freely available online

ISSN 2737-5323
Volume 2 Issue 2
https://www.iikii.com.sg/journal/AFM
Applied Functional Materials

Article

Modeling of Optical Characteristics of Silver Nanoparticles—Water Suspension Subject to Electromagnetic Irradiation

Hamid Reza Dehghanpour

Department of Physics, Tafresh University, Tafresh, Iran; h.dehghanpour@aut.ac.ir; Tel.: +988636241288

Received: May 20, 2022; **Accepted:** Jun 20, 2022; **Published:** Jun 30, 2022

Abstract: Electromagnetic radiation on the suspension of silver-water nanoparticles was simulated using Maxwell equations and the phenomenological equation of extinction crosssection and application of appropriate boundary conditions for nanoparticles with spherical geometry. The outputs of this simulation (extinction coefficient in different conditions) were compared with previous experimental results. The similarity between the simulation outputs and the experimental results indicates the high degree of reliability of the simulation method to predict the results of situations in which there is no experimental data.

Keywords: Electromagnetic radiation, Ag nanoparticles, Extinction coefficient

1. Introduction

From an optical point of view, the scattering and absorption of electromagnetic waves by nanostructures gave rise to theories such as Rayleigh theory, Rayleigh Gans theory, and Lorentz Mie theory. When a liquid heats up quickly, a semi-stable state is created to boil it to a temperature much higher than the normal boiling point temperature. The evaporation reaction, then, may cause an explosive and rapid state. When a pulsed laser heats metal nanoparticles in a suspension, solid and liquid bubbles are created on the joint surface, which results in sudden boiling. In this case, high heat is measured at a temperature of about 92% of the lattice temperature [1]. It is shown that a thin layer of vapor is formed in the vicinity of the nanoparticles and has a great effect on heating the particle surface in less than 100 ps. Laboratory examination of excessive heat and sudden boiling is performed and recorded at a microscopic resolution [2]. Time separation optical recorded experiments show that the energy absorbed by very short laser pulses is transmitted by electrons in the metal. The optical properties of metal nanoparticles can be adjusted by controlling their size and shape. In fact, Metal nanoparticles support the resonance of surface plasmons. They are highly dependent on geometry and the environment. Figure 1 shows the interaction of a laser beam with a nanoparticle and the creation of nanobubbles with shock waves.

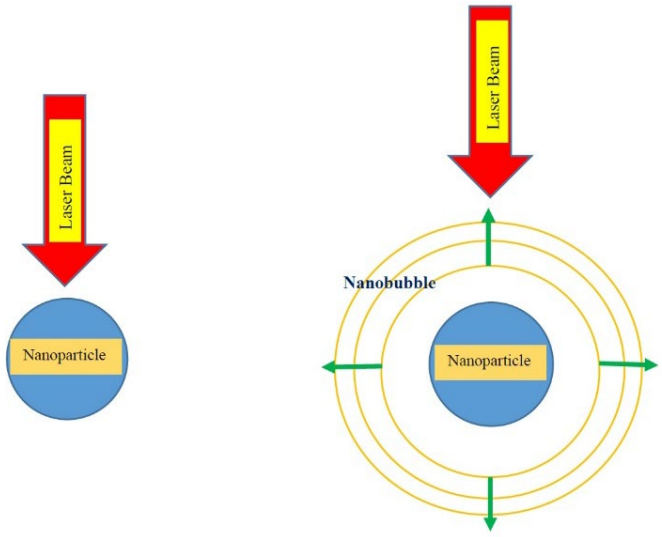

Fig.1. Schematic diagram of laser beam interaction with nanoparticles in a liquid environment.

2. Theory

The dielectric function is a complex function that expresses the response of matter to the electromagnetic field applied to it. The dielectric function describes the macroscopic properties of a solid. The dielectric function has two in-band shares that are used for metals. This function is shown as follows.

$$\varepsilon(\omega) = \varepsilon_1(\omega) + i\varepsilon_2(\omega) \tag{1}$$

In generalized Lorentz-Mai theory, by solving Maxwell equations, the answers are divided into two modes, transverse magnetic (TM) and transverse electric (TE). In this study, the relationships obtained from this theory are specifically used for spherical nanoparticles and spherical Gaussian waves. After completely solving the Maxwell equations under conditions with the properties of a spherical particle and applying suitable boundary conditions, complex quantities called the classical Mie dispersion coefficients are obtained as follows [3].

$$\begin{aligned} a_n &= \frac{M\Psi_n(Mx)\Psi_n'(x) - \Psi_n(x)\Psi_n'(Mx)}{M\Psi_n(Mx)\xi_n'(x) - \xi_n(x)\Psi_n'(Mx)} \\ b_n &= \frac{\Psi_n(Mx)\Psi_n'(x) - M\Psi_n(x)\Psi_n'(Mx)}{\Psi_n(Mx)\xi_n'(x) - M\xi_n(x)\Psi_n'(Mx)} \end{aligned} \tag{2}$$

In these equations, M determines the ratio of the refractive index of the particle to the refractive index of the environment. However, in the mentioned relations, the refractive index of the particle due to the metal structure of these particles, the complex number, and the refractive index of the surrounding environment is assumed to be real. Also, the x parameter, which is known as the size parameter, is defined as follows [4].

$$x = \frac{2\pi a n_m}{\lambda} \tag{3}$$

ξ_n and Ψ_n are called Ricati-Bessel relations and the prime sign indicates the derivative relative to the corresponding identifier, n_m is the refractive index and a is the radius of the spherical nanoparticles. By using complex scattering coefficients, the quantities that determine the amount of energy loss are expressed. These quantities, known as the absorption and extinction scattering cross sections, are shown as follows.

$$K_{sca} = \frac{\lambda^2}{\pi}\sum_{n=1}^{\infty}\sum_{m=-n}^{+n}\frac{(2n+1)(n+|m|)!}{n(n+1)(n-|m|)!}\{|a_n|^2|g_n^m, TM|^2 + |b_n|^2|g_n^m, TE|^2\} \tag{4}$$

$$K_{ext} = \frac{\lambda^2}{\pi}\sum_{n=1}^{\infty}\sum_{m=-n}^{+n}\frac{(2n+1)(n+|m|)!}{n(n+1)(n-|m|)!}Re\{|a_n|^2|g_n^m, TM|^2 + |b_n|^2|g_n^m, TE|^2\} \tag{5}$$

$$K_{abs} = K_{ext} - K_{sca} \tag{6}$$

Equations (4) to (6) represent the cross-sections of dispersion, extinction, and adsorption in spherical nanoparticles, respectively. These cross-sections are specifically expressed for spherical nanoparticles exposed to a spherical Gaussian beam. These cross-sections are of great importance in optical studies of metallic or even non-metallic nanoparticles because of their greater capabilities than the cross-sections of the classical Lorentz-Mie theory.

3. Results and Discussion

Due to the importance of the dielectric function of a substance that is affected by laser pulses, the nanoparticle-dielectric function diagrams of the relational excitation wavelength for its real and imaginary parts are shown as follows. The real and imaginary properties of this function are plotted in terms of wavelengths (Figs. 2 and 3), which agree well with the experimental diagrams [5].

$$\begin{aligned} \varepsilon_m &= 3500/\lambda - 3.75 \\ \varepsilon_r &= \left(-2.37\times10^{-7}\lambda^2\right) - 1.97 \end{aligned} \tag{7}$$

Both the real and imaginary parts of the dielectric function of nanoparticles decrease relatively smoothly with increasing wavelength. This suggests that adsorption and scattering by silver nanoparticles occur at greater near-red wavelengths.

$$\sigma_{ext} = \frac{9V\varepsilon_m^{\frac{3}{2}}\omega\varepsilon_2(\omega)}{c(\omega_1(\omega) + 2\,\varepsilon_m)^2 + \,\varepsilon_2\,(\omega)} \tag{8}$$

In this relation, V is the total volume of nanoparticles, ε_1 and ε_2 are the real and imaginary parts of the dielectric function of the environment containing nanoparticles, ε_m is the imaginary part of the dielectric function of nanoparticles, ω is the frequency of incident radiation and c is the speed of light in free space.

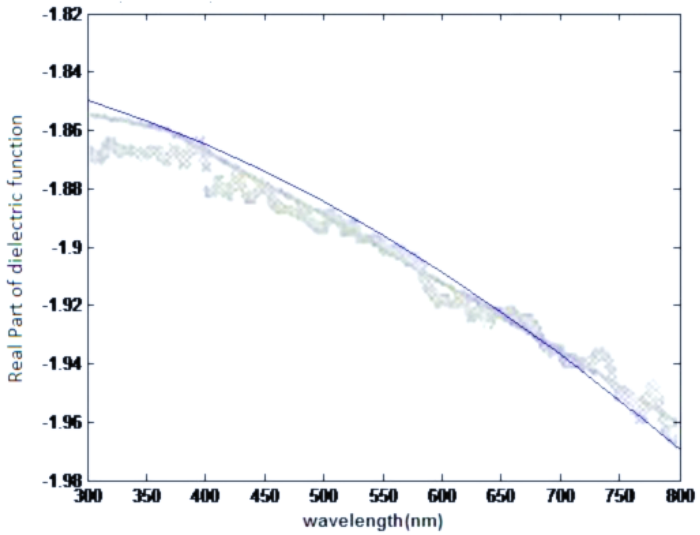

Fig. 2. Real part of the dielectric function of silver nanoparticles (continuous curves are the result of simulation and discrete data are experimental results).

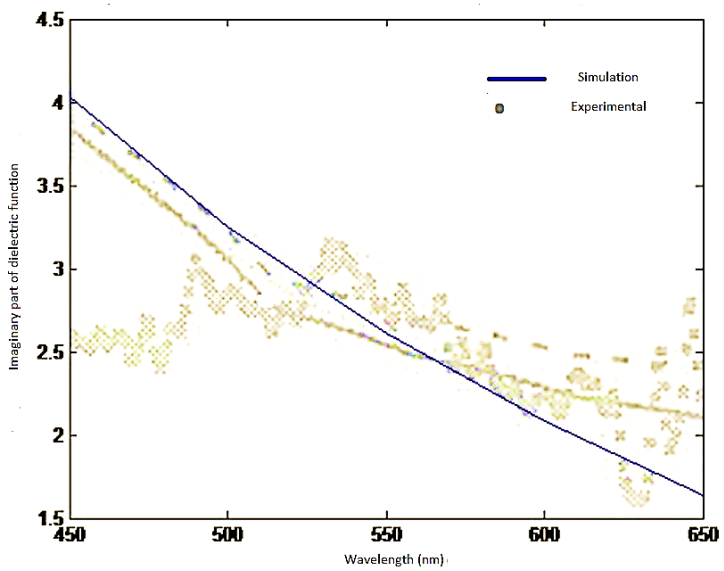

Fig. 3. Imaginary part of the dielectric function of silver nanoparticles (continuous curves are the result of simulation and discrete data are experimental results).

As shown in Fig. 4, at a constant wavelength of 400 nm, we observe a marked upward trend in the extinction cross-sectional area as the radius of the nanoparticles increases. Figure 5 shows the growth of the extinction crosssection with increasing wavelength to a wavelength of about 700 nm. As the wavelength increases, this crosssection takes a decreasing trend. As the radius of these

nanoparticles increases, we encounter an increase in the number of conducting electrons, which in turn reduces the penetration of the electric field into each of the nanoparticles. The consequence is that the electric field in these nanoparticles has only a surface penetration that causes surface effects. This, in turn, leads to heterogeneity in the distribution of the inner conducting electrons of nanoparticles. The heterogeneous distribution of free electrons within nanoparticles leads to the creation of bipolar, quadrupole, and octopus plasmonic peaks in the dispersion, adsorption, and extinction of nanoparticles [6].

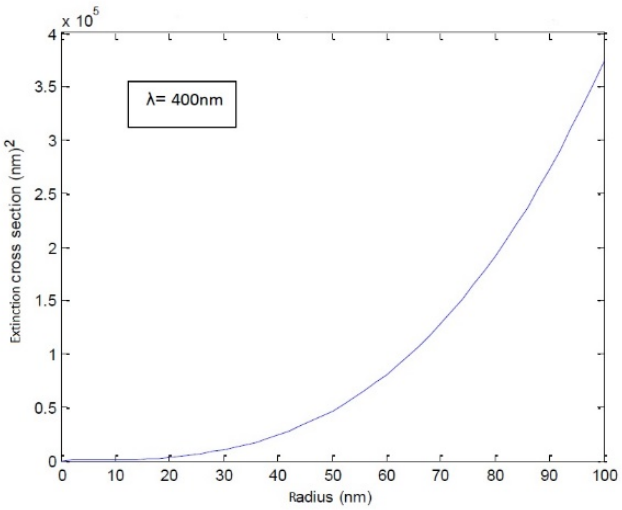

Fig. 4. Results of simulation of blackout cross section (K_{ext}) for different radii of silver nanoparticles at 400 nm incident wavelength.

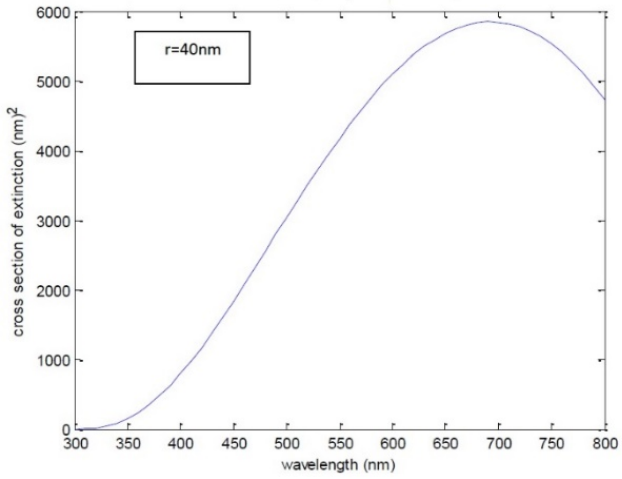

Fig. 5. Extinction cross-section simulation results (K_{ext}) for different incident wavelengths for a radius of 40 nm silver nanoparticles.

4. Conclusion

By using the solutions of Maxwell equations and applying suitable boundary conditions for metal nanoparticles under electromagnetic radiation, one of the important optical responses of the nanoparticles (extinction coefficient) was calculated, and the results obtained by simulation for silver nanoparticles were compared with available experimental results. This comparison showed that the modeling outputs performed coincided with the experimental results.

Funding: This research did not receive external funding.

Conflicts of Interest: The authors declare no conflict of interest.

References

1. Lang, F.; Leiderer, P. Phase transition dynamics measurements in superheated liquids by monitoring the ejection of nanometer-thick films. *Appl. Phys. Lett*. **2004**, *85*, 2759–2761.
2. Glod, S.; Poulikakos, D.; Zhao, Z.; Yadigaroglu, G. An investigation of microscale explosive vaporization of water on an ultrathin Pt wire. *Int. J. Heat Mass Transfer* **2002**, *45*, 367–379.
3. Plech, A.; Wulff, M.; Kuerbitz, S.; Berg, K.-J.; et al. Time-resolved X-ray diffraction on laser-excited metal nanoparticles. *Europhys. Lett*. **2003**, *61*, 762–768.
4. Johnson, P.B.; Christy, R.W. Optical Constants of the Noble Metals. *Phys. Rev. B* **1972**, 6, 4370–4379.
5. Malynych, S.; Moroz, I.; Kurlyak, V. Optical extinction spectra of aqueous suspensions of Ag nanopsarticles. *Ukr. J. Phys. Opt*. **2007**, *8*, 54–59.
6. Sönnichsen, C.; Franzl, T.; Wilk, T.; von Plessen, G.; Feldmann, J. Plasmon resonances in large noble-metal clusters. *New J. Phys*. **2002**, *4*, 93.